NOISE ROBUST LOCAL PHASE COHERENCE BASED METHOD FOR IMAGE SHARPNESS ASSESSMENT

Damir Seršić and Ana Sović

University of Zagreb, Faculty of Electrical Engineering and Computing, Croatia

ABSTRACT

Image sharpness assessment is a very important issue in image acquisition and processing. Novel approaches in no-reference image sharpness assessment methods are based on local phase coherence (LPC), rather than edge or frequency content analysis. It has been shown that the LPC based methods are closer to human observer assessments.

In this paper, we propose carefully designed complex wavelets that provide a good tool for the local phase estimation. Moreover, we take a special care of noise. We apply thresholding in the wavelet domain and merge several estimates to achieve statistical robustness in the presence of noise. It results in the sharpness index that over-performs previously reported methods.

Index Terms — complex wavelet transform, local phase coherence, image sharpness assessment, image blur

1. INTRODUCTION

Signal or image denoising, with a special emphasis on edge preservation is an often subject of research [1][2][3]. Although peak signal to noise ratio is widely used for validation of the results, the real benefit of the proposed methods is in precise restoration of details and sharp parts of images. Various algorithms have been proposed to measure image sharpness without known reference. They can be classified into three classes: edge, pixel and transform based methods [4].

Edge based methods usually detect edges or slope and gradient of the edges in an image. One simple approach is to identify vertical edges in the image and calculate average edge width [5]. Narvekar and Karam detect the edges and estimate a probability of detecting blur at the detected edges. The final cumulative probability of blur detection is calculated from a probability density function for the obtained probabilities [6].

Pixel based methods work in the spatial domain. They are based on the statistical properties and correlation between the pixels [7] and do not make assumptions about the edges. Zhu and Milanfar calculate singular value decomposition of the local image gradient matrix. Singular values reflect the strengths of the gradients along the dominant and its perpendicular direction. Therefore, they are sensitive to sharpness and could be used to measure it [8].

Some transform based methods rely on the fact that sharper edges increase the high frequency components [7][9]. Sharpness could be estimated on the histogram of non-zero discrete cosine transform coefficients among 8 x 8 blocks of the transformed image [10]. The overall sharpness estimate is given by the average of the sharpness values. In [11] the authors identified blur spectrum parameters for blind restoration of linearly moved or out-of-focus images. In [12] concept of global phase coherence based on discrete Fourier transform is introduced for image sharpness assessment. Another approach is based on using a complex wavelet transform. Local phase coherence (LPC) in the complex wavelet domain is computed at each spatial location to build a LPC map. Overall sharpness index is calculated via a weighted sum of the LPC map values [13][14]. The pioneering work of Hassen, Wang and Salama has inspired the approach presented in this paper.

We propose use of carefully time-domain designed complex wavelets to achieve maximum performance. Designed wavelets are short, odd sized and compactly supported, which provides for a precise instrument for local phase coherence analysis. The phase estimators are known to be very sensitive to noise. At first, we apply a thresholding method in the wavelet domain to distinguish between accurate and non-accurate local phase estimates. Then we use a set of estimators and combine their results across the scales and local neighborhoods to achieve robust LPC estimates. Finally, we propose a sharpness index in more intuitive way than in [13].

This paper is organized as follows. Section II provides a theoretical background of the local phase coherence and proposed method for noisy signals. In Section III, we present the experimental results. General conclusions are presented in Section IV.

2. LOCAL PHASE COHERENCE

One dimensional continuous wavelet transform of signal $f(t)$ is:

$$F(a, \tau) = \frac{1}{\sqrt{|a|}} \int_{-\infty}^{\infty} f(t) \, \psi^* \left(\frac{t - \tau}{a} \right) dt, \tag{1}$$

where a is a scale and τ is a position. As a mother wavelet function, we propose to use a short complex function $e^{j\omega_0 t}$ on a single period $2\pi/\omega_0$:

$$\psi(t) = \left[\mu \left(t + \frac{\pi}{\omega_0} \right) - \mu \left(t - \frac{\pi}{\omega_0} \right) \right] e^{j\omega_0 t} \tag{2}$$

where $\mu(t)$ is the unit step function.

Human observer assessment of sharpness is often focused on well spatially localized signal or image elements. The typical representatives are discontinuities: impulses, steps, or edges in images. In the sequel, we show that well localized signals exhibit very convenient local phase coherence property across the wavelet scales.

For the impulse $f(t) = K\delta(t - t_0)$, the wavelet transform on position t_0 is:

$$F(a, \tau) = \frac{K}{\sqrt{|a|}} e^{-j\omega_0 \frac{t_0 - \tau}{a}},$$
$$\text{for } \tau - \frac{\pi}{\omega_0} a < t_0 < \tau + \frac{\pi}{\omega_0} a. \tag{3}$$

The phase of $F(a, \tau)$ is:

$$\measuredangle \big(F(a, \tau) \big) = \begin{cases} \omega_0 \dfrac{\tau - t_0}{a}, & \text{for } K \geq 0, \\ \omega_0 \dfrac{\tau - t_0}{a} + \pi, & \text{for } K < 0. \end{cases} \tag{4}$$

For the step function $f(t) = K\mu(t - t_0)$ the wavelet transform on position t_0 is:

$$F(a, \tau) = \frac{Ka}{\sqrt{|a|}\omega_0} \cos \left(\omega_0 \frac{t_0 - \tau}{2a} \right) e^{j \left(\omega_0 \frac{t_0 - \tau}{2a} - \frac{\pi}{2} \right)},$$
$$\text{for } \tau - \frac{\pi}{\omega_0} a < t_0 < \tau + \frac{\pi}{\omega_0} a. \tag{5}$$

and the phase of $F(a, \tau)$ is:

$$\measuredangle \big(F(a, \tau) \big) = \begin{cases} \omega_0 \dfrac{\tau - t_0}{2a} - \dfrac{\pi}{2}, & \text{for } K \geq 0, \\ \omega_0 \dfrac{\tau - t_0}{2a} + \dfrac{\pi}{2}, & \text{for } K < 0. \end{cases} \tag{6}$$

From (4) and (6), a linear phase relationship across scale and space stands for ideally localized features in the scale-position domain:

$$\measuredangle \big(F(a, \tau) \big) = k_1 \omega_0 \frac{\tau - t_0}{a} + k_2 \frac{\pi}{2}, \tag{7}$$

where integer constant k_1 is 1 for the impulse, and ½ for the step function. Furthermore, an integer constant k_2 is 0 for the positive impulse, 2 for the negative impulse, -1 for the ascending step edge and +1 for the descending step edge.

Wavelet analysis across a set of scales a result in locally linear phase segments (Eq. 7) that intersect in a single point (Fig. 1), which correspond to a strong local linear phase coherence. Hence, the LPC can be used either for discontinuity detection, or for sharpness assessment.
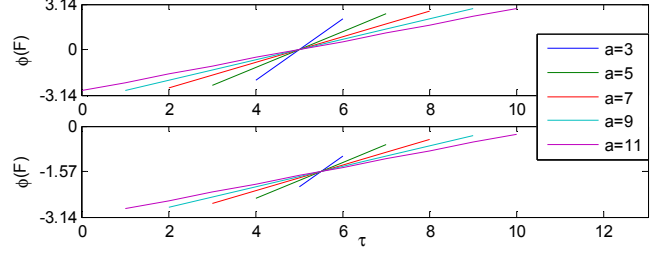

Fig. 1. Example of local phase coherence: (a) phase of the impulse $\delta(t - 5)$ in the complex wavelet domain for different scales; (b) phase of the step function $\mu(t - 6)$ in the complex wavelet domain for different scales. The phases are intentionally displayed as continuous functions, for the visibility.

In practical implementation, discrete wavelet transform is used. Therefore, the wavelet function (2) must be sampled. We regard (2) as a projection of a unit vector in a complex plane that rotate one full circle. Hence, we took samples of $\psi(t)$ on the unit circle split to equidistant angles. Our proposal is to use odd lengths of the filters ($N = 3, 5, 7, 9$ and 11), centered around zero angle. It corresponds to scales $a = 3/3, 5/3, 7/3, 9/3$ and $11/3$. Hence, sum of discrete filter coefficients $\psi(n)/\sqrt{a}$ is zero, which makes it admissible for the wavelet analysis. Moreover, the filters are centered on samples 2, 3, 4, 5 and 7, respectively. Counter clockwise rotation produces discrete wavelet $\psi_+(n)$, and clockwise rotation gives $\psi_-(n) = conj(\psi_+(n))$. For the completeness, we denote low pass filter as $\psi_0(n) = 1/\sqrt{a}$, for each n. Short, compactly supported wavelets provide for a precise tool for the local phase analysis.

Examples of phases of well localized signals (impulse $\delta(t - 5)$ and step $\mu(t - 6)$) are shown in Fig. 1. Linear phase relationship is clearly visible. Local phases for all wavelet scales intersect in a single point. If the signal is blurred (e.g. low-pass filtered), the phases are not linear. Therefore, we can measure the sharpness by examining the linearity and the coherence of its local phases.

The proposed wavelet function is generalized in 2D:

$$\psi_o(m, n) = \psi_k(m) \times \psi_l(n), \tag{8}$$

where $\times$ denotes outer product and $k, l \in \{-, 0, +\}$. It produces 9 spatial orientations o. The local phase is calculated for each pixel and for all scales under consideration. If the image has sharp edges, linear phase coherence is clearly visible, while for blurred edges phases are not linear and do not intersect in a single point.

The strength of the LPC can be measured by calculating similarity between the ideal linear phase and the actual phase in the observed signal or image. Since, we do not have the ideal signal the ideal linear phase must be estimated. One approach is based on the fact that the finest scale coefficients can be well predicted from the coarser scale coefficients in the neighboring positions [15]. The other approach fixes the position τ in the scale-position domain and minimizes an error function that depends on the scales [13]. Our proposed method is based on the second approach and presented in the sequel.

2.1. Phase prediction

Our goal is to maximize a similarity measure between the true and estimated ideal phase samples. We define the LPC strength measure as:

$$S_{LPC} = \left(\pi - \left|\mathbf{w}^T\boldsymbol{\Phi} - \mathbf{w}^T\widehat{\boldsymbol{\Phi}}\right|^p\right)/\pi, \tag{9}$$

where $\boldsymbol{\Phi}$ is a vector of the measured phases, and $\widehat{\boldsymbol{\Phi}} = \left[\angle\left(F(a_1,\tau_1)\right) \ \ \angle\left(F(a_2,\tau_2)\right) \ \ ... \ \ \angle\left(F(a_N,\tau_N)\right)\right]^T$ is the vector of the ideal values of the phases from (7). Exponent p can be set to match desired error surface shape. In the rest of the paper it will be set to 1. If we can find a set of weights $\mathbf{w}$ and a set of samples $\widehat{\boldsymbol{\Phi}}$ such that

$$\mathbf{w}^T\widehat{\boldsymbol{\Phi}} = 0, \tag{10}$$

the measure of the LPC is simplified:

$$S_{LPC} = (\pi - |\mathbf{w}^T\boldsymbol{\Phi}|)/\pi. \tag{11}$$

It is important to mention that in [13] the authors were using a cosine based similarity measure, followed by some extra steps for eliminating negative values. We believe that proposed (11) is an intuitive measure directly derived from (10). The phase is in radians, and for perfect edges product $\mathbf{w}^T\boldsymbol{\Phi}$ tends to zero. Eq. (11) produces results in range [0, 1], where 1 corresponds to a perfectly sharp edge.

In order to calculate the weight vector, we extract N samples in the scale-position domain at the same position τ and at different scales. Further, we substitute (7) into (10):

$$k_1\omega_c(\tau - t_0)\sum_{i=1}^{N}\frac{w_i}{a_i} + k_2\frac{\pi}{2}\sum_{i=1}^{N}w_i = 0. \tag{12}$$

It is important to notice that the right term of (12) provides for linear shift and thus phase wrapping insensitive results. We minimize energy of the weights $E = \sum_{i=1}^{N}w_i^2$, under the constraints $\sum_{i=1}^{N}\frac{w_i}{a_i} = 0$ and $\sum_{i=1}^{N}w_i = 0$, similar to [13].

Since we use predefined scales, we can calculate the weights in advance. For scales 3/3, 5/3, 7/3, 3 and 11/3, the weights are:

$$\mathbf{w}_{\{5\}} = [1 \ \ -2.10 \ \ -0.44 \ \ 0.48 \ \ 1.06]^T.$$

More scales provide for more reliable estimates. But, longer filters demand for bigger neighborhood of the observed point or pixel, which is not necessarily available (Section 2.2). Hence, we propose to use a set of estimators that uses reduced number of scales. For scales 5/5, 7/5, 9/5, 11/5, the weights are:

$$\mathbf{w}_{\{4\}} = [1 \ \ -2.06 \ \ -0.10 \ \ 1.16]^T,$$

and for scales 7/7, 9/7, 11/7, the weights are:

$$\mathbf{w}_{\{3\}} = [1 \ \ -2.57 \ \ 1.57]^T,$$

where indices {5}, {4} and {3} denote the number of involved scales, as well as their corresponding weights.

We calculate the LPC strength measure for o-th orientation and k-th location using (11) and one of the predefined weights:

$$S_{LPC}^{\{o,k\}} = \left(\pi - \left|\sum_{i=1}^{N}w_i \cdot \angle\{c_i\}\right|\right)\Big/\pi, \tag{13}$$
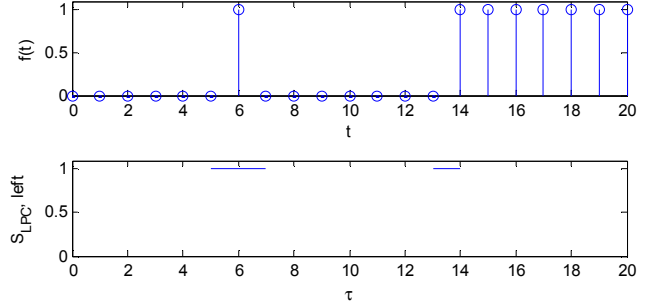

Fig. 2. LPC strength measure for 1D signal: (a) signal, (b) S_{LPC} for positive (or "left") orientation.
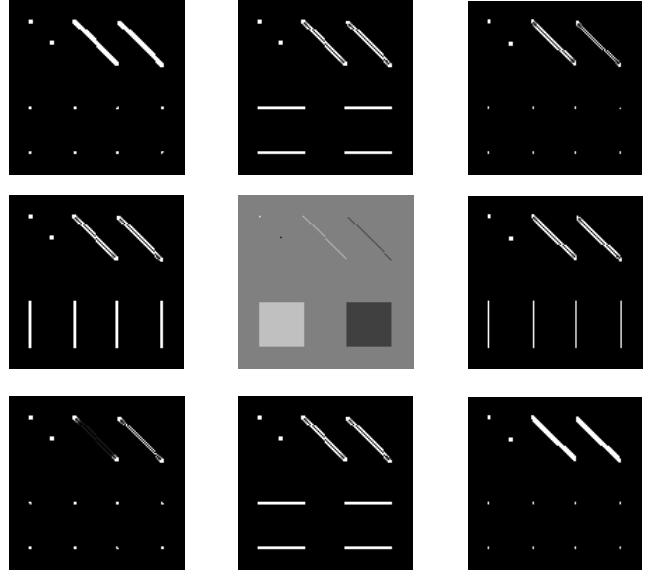

Fig. 3. LPC strength measure of an artificial image (center). S_{LPC} for eight orientations are on corresponding places (low - low component is avoided).

where $c_i = F(a_i, \tau)$ are the complex wavelet coefficients at the i-th scale and at every observed location τ.

LPC strength measure is calculated for each orientation o and for each position k in the 1D signal or in the image. Examples are given in Fig. 2 and Fig. 3. The results strongly depend on the orientation of edges in images.

In the presence of noise, it is more difficult to reliably estimate the phase. To reduce the unwanted impact of the noise on sharpness decision, we combine several LPC strength maps to find a better estimation of the phase.

2.2. Phase prediction in the presence of noise

At first, to minimize the influence of the noise in phase estimation, we introduce thresholding in the wavelet domain. Let σ be standard deviation of Gaussian zero mean noise added to the input signal $f(t)$. In our experiments, we set threshold value to a conservative level $\gamma = 3\sigma$. However, the threshold parameter could be optimally chosen for each image individually. If

$$|F(a,\tau)| < \gamma, \qquad (14)$$

we consider phase estimate as non-accurate and do not take it into the account. Otherwise, we calculate our LPC strength measures. If phase estimates for all 5 scales are available according to (18) at some observed position τ, we calculate LPC strengths using weights $\mathbf{w}_{\{5\}}$:

$$S_{LPC}^{\{o,k\}} = \left(\pi - \left|\mathbf{w}_{\{5\}}{}^T \mathbf{\Phi}_{\{5\}}\right|\right)/\pi. \qquad (15)$$

Else, if only 4 scales are available, using weights $\mathbf{w}_{\{4\}}$ we calculate the LPC strengths measure:

$$S_{LPC}^{\{o,k\}} = \left(\pi - \left|\mathbf{w}_{\{4\}}{}^T \mathbf{\Phi}_{\{4\}}\right|\right)/\pi. \qquad (16)$$

Finally, if only 3 scales are available, we use the shortest LPC strength estimate:

$$S_{LPC}^{\{o,k\}} = \left(\pi - \left|\mathbf{w}_{\{3\}}{}^T \mathbf{\Phi}_{\{3\}}\right|\right)/\pi. \qquad (17)$$

But, in the presence of noise, the estimation of phase $\mathbf{\Phi}$ is not ideal (Fig. 4). To get a more confident estimation of the LPC strength, we propose use of weighted moving average of the LPC strength maps:

$$S_{LPC}^{\{o,k\}} = \frac{\sum_{n=k-K/2}^{k+K/2}|F(1,\tau_n)|^2 \cdot S_{LPC}^{\{o,n\}}}{\sum_{n=k-K/2}^{k+K/2}|F(1,\tau_n)|^2}. \qquad (18)$$

If $|F(a,\tau)| \gg \sigma$, then $\sigma_{phase}^2 \approx \sigma^2/|F(a,\tau)|^2$. Hence, a minimum variance phase estimate is a weighted average of neighboring estimates with weights set to $1/|F(a,\tau)|^2$, which results in (18). Wavelet coefficients from the shortest filters are used: $F(1,\tau)$. 2D generalization uses rectangular moving window derived from (18) in a straightforward way.

2.3. Spatial LPC map

Spatial LPC map is a collection of all LPC strength maps for all observed orientations. In [13], a weighted average was used. Instead, we propose:

$$S_{LPC}^{\{k\}} = \max\left(S_{LPC}^{\{o,k\}}\right), \qquad (19)$$

where LPC maps for different orientations are denoted with o, where $o = 1,2$ for 1D signals and $o = 1, 2, \dots, 8$ for images. In the case of sharp objects, the edge is often strong in only one orientation, and therefore it is not visible in all LPC strength maps (Fig. 3). However, using the maximum pooling corresponds to our goal: construction of sharpness measure.

3. EXPERIMENTS

Except for synthetic images, we applied the proposed method on the real world images. The results are shown in Fig. 6. The second column corresponds to the results of [13]. The third column illustrate the benefits of the proposed wavelets: the resulting LPC maps are sharp, precisely reflecting the image edges and fine details. Hence, our robust LPC estimate can be used as an edge & discontinuities detector. The right-most column shows the proposed averaged spatial LPC maps, robust to noise. The maps can be used for a reliable assessment of image sharpness, where accurate phase estimates contribute to the overall results.
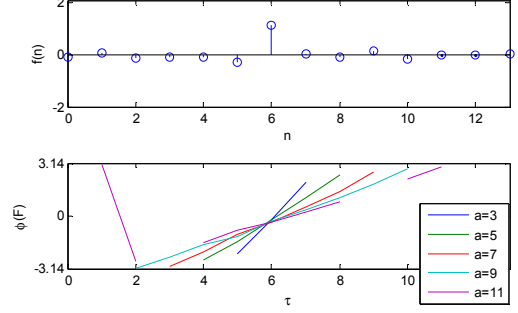

Fig. 4. Example of phase coherence for a noisy input signal. Top to bottom: noisy impulse, phase estimates for different scales.

Fig. 5. Spatial LPC map of the noiseless synthetic image.

	S_{LPC} from [13]	$S_{LPC,\{5\}}$	S_{LPC}
hats	0.923	0.243	0.871
noisy hats	0.914	0.255	0.917
blurred hats	0.904	0.091	0.451
blurred noisy hats	0.879	0.056	0.431

Table 1. Sharpness index for images in Fig. 6 using default $\beta = 10^{-4}$ for [13], and $\beta = 0.05$ for the proposed methods.

For image sharpness assessment, we use a sharpness index derived from [13] and proposed (19): $\gamma = \sum_{k=1}^{K} u_k S'_{LPC}^{\{k\}} / \sum_{k=1}^{K} u_k$, where $S'_{LPC}^{\{k\}}$ is $S_{LPC}^{\{k\}}$ sorted in descending order, $u_k = \exp\{-(k-1)/[(K-1)\beta]\}$, β is predefined constant (Table 1) and K is the signal size. Exact numbers for images in Fig. 6 are given in Table 1. For the proposed method, values of γ are clearly different for sharp and blurred images, which was not the case in [13]. The results are robust to noise. Comparison with subjective human evaluation is left for future research.

CONCLUSION

Local phase coherence is a very promising construct for assessment of image sharpness. In this paper, a careful design of discrete complex wavelets for this purpose is presented. A noise robust LPC estimate is based on thresholding and merging of individual phase estimates on different scales, orientations and local neighborhoods.

The weighted moving average approach uses such weights to achieve minimum phase estimation variance in the presence of noise, which was not considered in previous work [13]. The results are promising and superior in the noisy conditions.
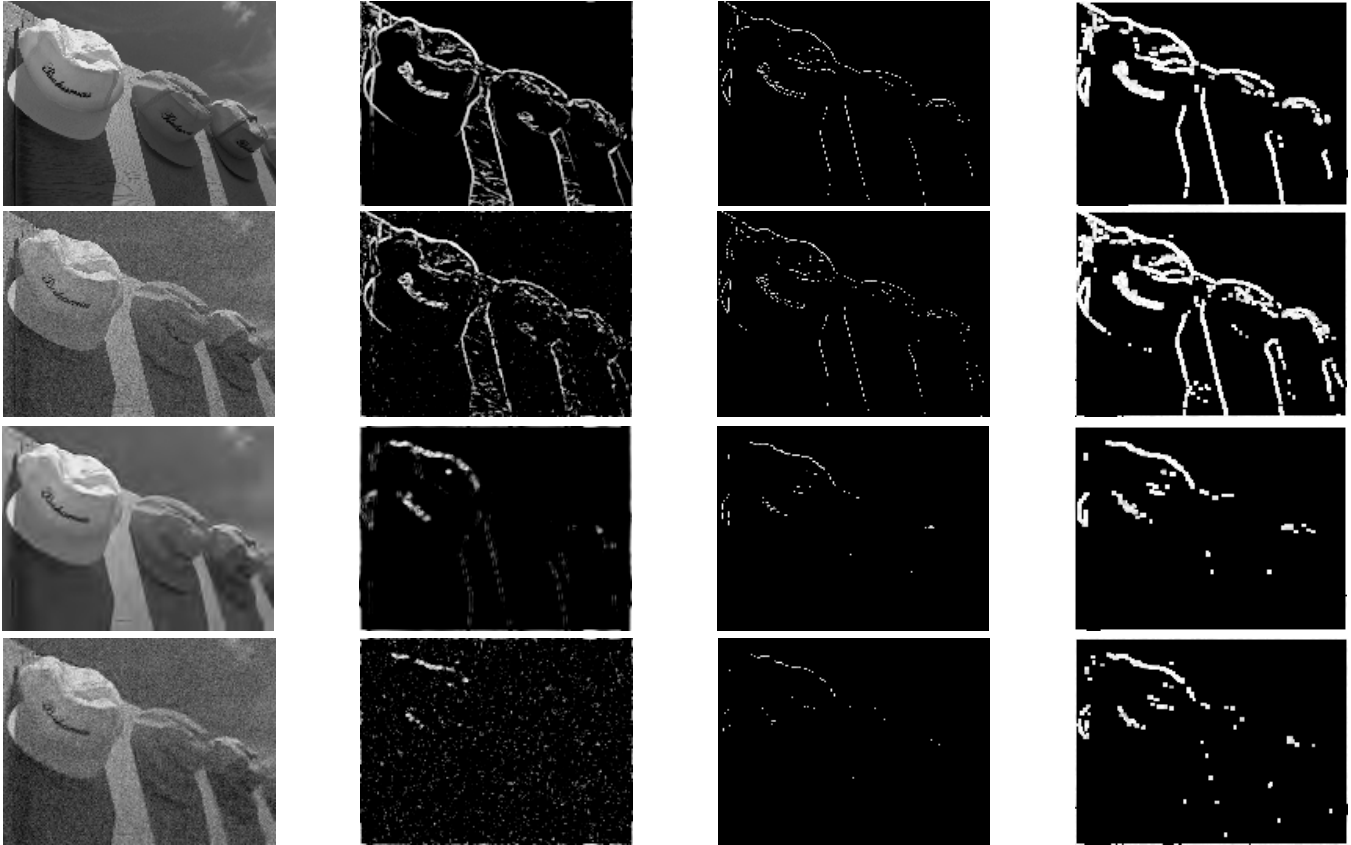
Fig. 6. Columns left to right: noisy real-world image, LPC map using [13], LPC map using $S_{LPC,\{5\}}$ only, LPC map using averaged S_{LPC}. Rows top to bottom: hats, noisy hats with $\sigma = 15$, blurred hats, blurred and noisy hats with $\sigma = 15$.

REFERENCES

[1] D. Seršić and A. Sović, "A robust improvement of the ICI rule for signal denoising," in *7th International symposium on image and signal processing and analysis*, pp. 26–31, 2011.

[2] M. Tomić and D. Seršić, "Adaptive edge-preserving denoising by point-wise wavelet basis selection," *IET Electronics letters signal processing*, vol. 6, no. 1, pp. 1–7, 2012.

[3] M. Tomić, S. Lončarić, and D. Seršić, "Adaptive spatio-temporal denoising of fluoroscopic X-ray sequences," *Biomedical Signal Processing and Control*, vol. 7, no. 2, pp. 173–179, 2011.

[4] C. T. Vu, T. D. Phan, and D. M. Chandler, "**S**_3 : A spectral and spatial measure of local perceived sharpness in natural images," *IEEE Transactions on Image Processing*, vol. 21, pp. 934–945, March 2012.

[5] P. Marziliano, F. Dufaux, S. Winkler, and T. Ebrahimi, "A no-reference perceptual blur metric," in *International Conference on Image Processing*, vol. 3, pp. 57–60, 2002.

[6] D. Narvekar and L. J. Karam, "A no-reference image blur metric based on the cumulative probability of blur detection (CPBD)," *IEEE Transactions on Image Processing*, vol. 20, pp. 2678–2683, Sept 2011.

[7] R. Ferzli and L. Karam, "A no-reference objective image sharpness metric based on the notion of just noticeable blur (JNB)," *IEEE Transactions on Image Processing*, vol. 18, pp. 717–728, April 2009.

[8] X. Zhu and P. Milanfar, "A no-reference sharpness metric sensitive to blur and noise," in *International Workshop on Quality of Multimedia Experience*, pp. 64–69, July 2009.

[9] A. Chetouani, A. Beghdadi, and M. Deriche, "A new reference-free image quality index for blur estimation in the frequency domain," in *IEEE International Symposium on Signal Processing and Information Technology (ISSPIT)*, pp. 155 – 159, 2009.

[10] X. Marichal, W.-Y. Ma, and H. Zhang, "Blur determination in the compressed domain using DCT information," in *International Conference on Image Processing*, vol. 2, (Kobe), pp. 386–390 vol.2, 1999.

[11] J. P. Oliveira, M. A. T. Figueiredo, and J. M. Bioucas-Dias, "Parametric blur estimation for blind restoration of natural images: Linear motion and out-of-focus," *IEEE Transaction on Image Processing*, vol. 23, no. 1, pp. 466–477, 2014.

[12] G. Blanchet and L. Moisan, "An explicit sharpness index related to global phase coherence," in *IEEE ICASSP*, pp. 1065–1068, 2012.

[13] R. Hassen, Z. Wang, and M. Salama, "Image sharpness assessment based on local phase coherence," *IEEE Transactions on Image Processin*, vol. 22, no. 7, pp. 2798 – 2810, 2013.

[14] R. Hassen, Z. Wang, and M. Salama, "No-reference image sharpness assessment based on local phase coherence measurement," in *IEEE ICASSP*, Dallas, Texas, USA, 2010.

[15] T. Wang and E. Simoncelli, "Local phase coherence and the perception of blur," in *Advances in Neural Information Processing Systems*, vol. 16, Cambridge, MA: MIT Press, 2003.